CHEMISTRY
A EUROPEAN JOURNAL

DOI: 10.1002/chem.200701744

Synthesis of Copper Dendrite Nanostructures by a Sonoelectrochemical Method

Iris Haas,[a] Sangaraju Shanmugam,[b] and Aharon Gedanken*[a]

Abstract: Copper dendrites have been prepared by a sonoelectrochemical process from an aqueous solution of Cu^{2+} in the presence of polyvinyl alcohol. A SEM image of the morpholohy of the copper formed on the electrode after one electric pulse is presented. A subsequent sonic pulse removes the copper from the electrode surface, cleaning it for the next step. The formation of the dendrites is accounted for by the "drying-mediated self-assembly of nanoparticles" theory.

Keywords: copper · dendrimers · nanostructures · polyvinyl alcohol · sonoelectrochemistry

Introduction

In recent years, much attention has focused on well-defined nanostructured metals, such as nanoparticles, nanocubes, nanotetrahedrals, nanowires, and nanorods, because of the influence of their size and shape on their electronic, optical and catalytic properties.[1,2] It is well-known that catalytic reactivity depends not only on the size of the metallic nanoparticles, but also on their shape.[3,1b] Therefore, the synthesis of colloidal particles with controlled shapes and sizes is important. Several synthetic methods have been employed for the preparation of colloidal metal solutions. These methods generally involve the reduction of the relevant metallic ion in the presence of a suitable surfactant, which is useful for controlling the growth of the metal particles.[4] There are already some reports on the synthesis of colloidal-metal solutions that contain Ag,[5–7] Au,[8] Pt,[9] Pd,[10] Zn,[11] and Cu[12] with a dendritic structure. The techniques employed in these reports include electrochemical deposition, vapor-phase polymerization, photoreduction by ultraviolet irradiation, pulse sonoelectrochemistry,[6,10] and a template approach.

Previous studies have shown that the growth of dendritic copper nanostructures can be achieved by an electrodeposition method without using a stabilizer.[12] Other studies have revealed that polyvinyl alcohol (PVA) plays a significant role in the formation and growth of Ag dendrites.[5] Rogach and co-workers have demonstrated that PVA forms a film-type polymeric matrix that stabilizes the Ag particles.[5b] In addition, nanostructure dendrites of Ag[6] and Pd[10] can be synthesized sonoelectrochemically by increasing the duration of the experiment.

Herein, we present a surfactant-assisted (PVA) sonoelectrochemical method for the fabrication of copper dendritic nanostructures. We have succeeded in obtaining a SEM image of the electrode after one electric pulse, before the material is removed from the electrode by the subsequent sonic pulse. This has allowed us to discuss and answer the question as to whether the dendritic structure obtained by sonoelectrochemistry is formed at one of the following three stages: 1) on the electrode (cathode) after the electrodeposition of the metallic copper, 2) in the solution after the removal of the copper from the electrode surface, and 3) on the TEM copper/carbon grid. The current investigation has also revealed that the sonoelectrochemical parameters, and the nanoparticle concentration and size, determine dendrite formation. It is worth noting that Nabiev and co-workers have also found that the formation of dendrites is dependent on the concentration of the nanoparticles.[2] We have used a model developed by Rabani and co-workers to explain the formation of the dendrites upon varying the various sonoelectrochemical parameters.[13]

[a] I. Haas, Prof. A. Gedanken
Department of Chemistry and Kanbar Laboratory for Nanomaterials at the Bar-Ilan University Center for Advanced Materials and Nanotechnology, Bar-Ilan University
Ramat-Gan, 52900 (Israel)
Fax: (+972) 3-7384053
E-mail: gedanken@mail.biu.ac.il

[b] Dr. S. Shanmugam
Institut für Anorganische Chemie (IAC)
RWTH Aachen, Landoltweg 1, 52074 Aachen (Germany)

Results and Discussion

Sonoelectrochemical process: In a previous paper[14] we described the same sonoelectrochemical technique as that used herein, but with poly(*N*-vinyl pyrrolidone) (PVP) as the stabilizer. In the previous study, many parameters were found that determine the size of the copper nanoproducts, herein we focus on the parameters that determine the shape of the nanoparticles. We found that a copper fractal structure was obtained in the sonoelectrochemical processes when the reaction was conducted in the presence of PVA (Figure 1). The size of the copper dendrites was around 1–2 μm. Figure 2 presents a typical high resolution TEM (HRTEM) image of the product. This TEM image presents a closer look at the dendrite morphology. These fractals consist of small copper particles the sizes of which are (8.5 ± 1.5) nm. Figure 2d depicts the HRTEM fringes of an individual copper particle obtained for a pulse width of 300 ms. The length of the lattice fringes was 0.208 nm, which corresponds well with the *d* value of the (111) plane of Cu^0 (0.208 nm according to JCPDS 4–836).

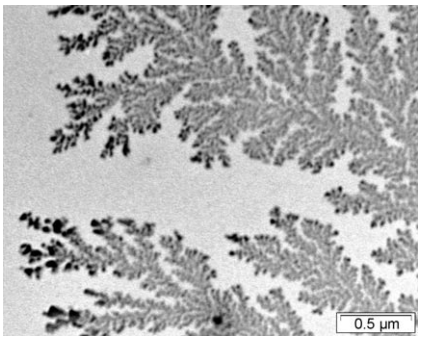

Figure 1. TEM image of the dendrite morphology observed for a current pulse width of 300 ms in the presence of PVA.

The sonoelectrochemical process is composed of a current pulse that is immediately followed by a sonic pulse. Because it is well-known from the literature that dendrites can be synthesized by an electrochemical process,[11] we began to analyze whether there is a relationship between the particles deposited on the electrode and the dendrite structure. We have examined the structure of the product formed after one electric pulse, namely, only the electrochemical process. This was done by capturing an SEM image of the electrode's surface after one electric pulse. The AFM image observed after one current pulse (without the subsequent sonic pulse) shows the formation of flowerlike structures deposited on the electrode (Figure 3); each flower is composed of 4–10 petals. The copper flowers in Figure 3 are synthesized by a current pulse with a width of 300 ms. The dimensions of this flower are $450 \times 175\ nm^2$. Figure 4 (top)

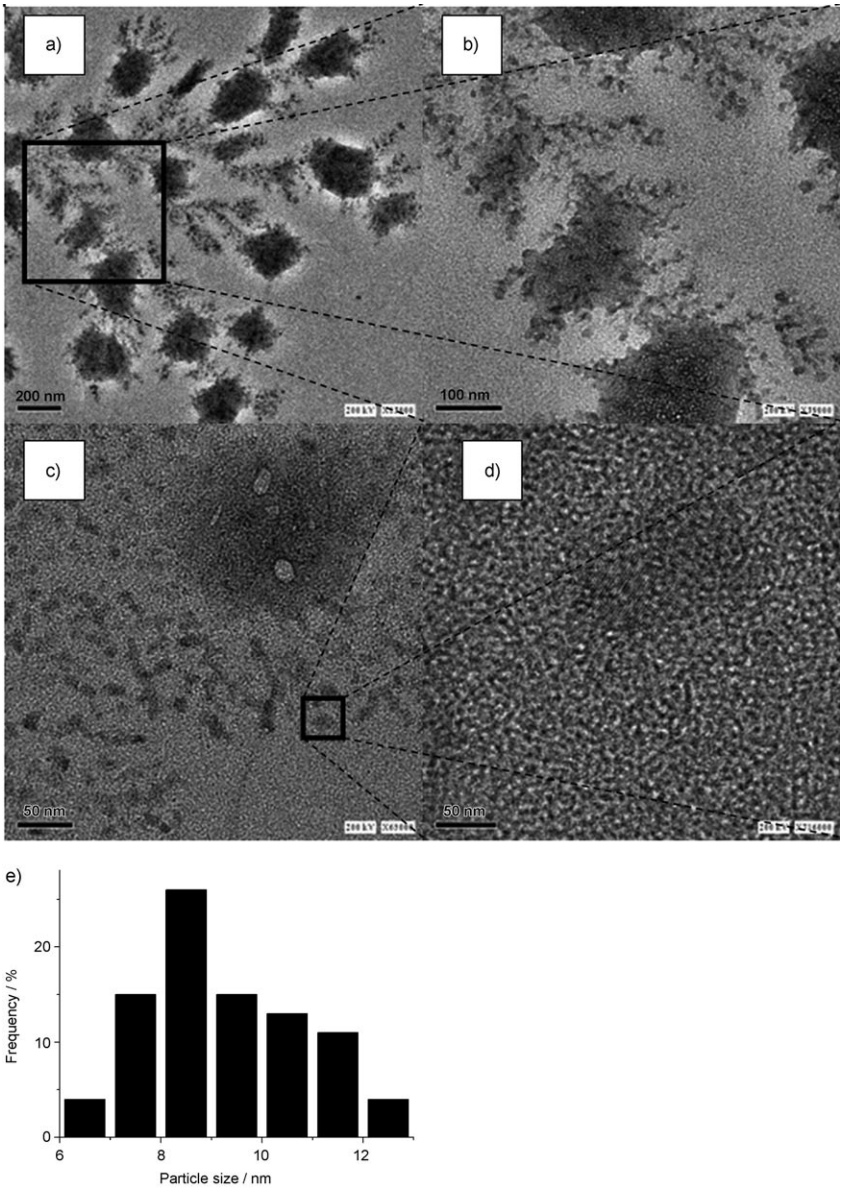

Figure 2. a–c) TEM images of copper dendrites synthesized at a current pulse width of 300 ms, d) fringes of an individual copper particle, and e) a histogram of the sizes of individual copper particles.

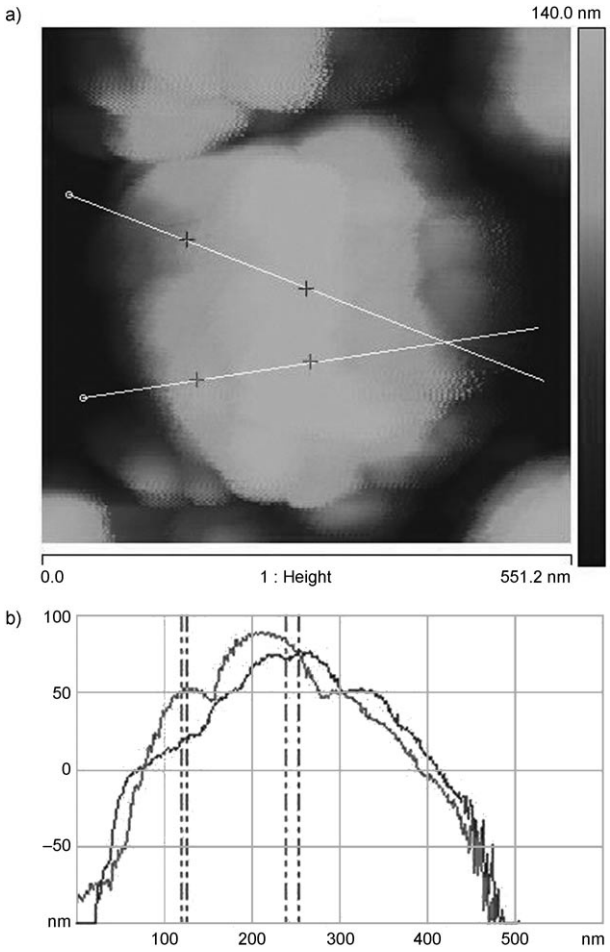

Figure 3. a) An AFM image of flowerlike structures deposited on the electrode after one electric pulse (300 ms wide). b) Morphological graph of the flowerlike structures.

shows SEM images of the flowers deposited on the electrode after one pulse of electricity had passed through the solution. The size of the flowers was measured as a function of the pulse width (Table 1).

It is observed that as the width of the current pulse increased, the size of the copper flowers also increased. When examining the flowers under high magnification, we found that each flower was constructed from small nanoparticles. In addition, as the current pulse width increased, the size of the copper nanoparticles increased. Further examinations of the flowers were performed to find out whether there are pores inside them. By using a surface-area analyzer (BET), it was found that the flowers do not contain pores and have very low surface areas ($2\ m^2 g^{-1}$). Low-angle XRD ($2\theta = 0.5$–$10°$) did not show any diffraction peaks assigned to mesopore or micropore formation, which confirmed that there are no pores inside the flowers. A SEM image taken after one electric pulse and one sonic pulse had passed through the solution revealed that the flowers were completely removed from the electrode by the sonic pulse. Thus, it was concluded that dendrites were not formed on the electrode. The experiments also indicate that, upon removal of the flowers from the electrode surface, they most probably disintegrate into individual nanoparticles.

We calculated the fractal dimensions of the dendrites as a function of two different parameters, namely, the duration of the sonoelectrochemical experiment (the current pulse width was kept constant at 300 ms) and the different electric pulse widths of the sonoelectrochemical experiment (the duration of the experiment was kept constant at 30 min). The fractal dimensions are 1.79 ± 0.02, 1.76 ± 0.02, and 1.75 ± 0.02 for the sonoelectrochemical runs of, 10, 20, and 30 min, respectively, or 1.75 ± 0.02 and 1.79 ± 0.02 for pulse widths of 300 and 400 ms. The results show that within the experimental error the fractal dimension is independent of the duration of the experiment or the pulse widths.

What remains to be elucidated is where the dendrites are formed. Are they formed on the TEM grid, or are they perhaps already formed in the solution? If they are formed on the grid, then perhaps their formation is dependent on

1) the nature of the substrate and/or
2) the size of the copper nanoparticles and/or
3) the concentration of the copper nanoparticles.

To address the first possibility, the solution obtained from the 300 ms pulse width, which produced a dendritic structure when deposited on the copper/carbon grid, was deposited on a gold grid. Figure 5a shows the TEM image, that resulted from this experiment. The TEM image from this experiment (Figure 5a) shows dispersed nanoparticles, which are spread all over the grid, rather than dendrites (33 ± 5) nm. In addition, this experiment was reproduced with the solution obtained from an 800 ms current pulse width. The general features of the TEM image were similar to those obtained for the 300 ms pulse. The dispersed nanoparticles (29 ± 5) nm were spread all over the grid and no dendrites were formed. These experiments clearly show that the nature of the grid and the nanoparticles determine whether dendrites will be formed.

Additional experiments were carried out to clarify the second possibility, that is, whether the size of copper nanoparticles encourages dendrite formation. Sonoelectrochemical formation of a dispersion of copper nanoparticles from solution was studied by varying the different parameters, namely, current and current pulse width, that control particle size. Before addressing the second possibility in more detail, results of size-related experiments will be presented.

Figure 6 shows the absorbance spectra of aqueous colloidal solutions of copper nanoparticles. An absorption band at 590 nm was observed that is due to the surface plasmons of the copper nanoparticles. It is well-known that colloidal solutions of metallic nanoparticles exhibit absorption bands in the UV/Vis region due to collective excitations of their free electrons (surface plasmon band).[14,15] The current flowing through the sonoelectrochemical cell affects the surface plasmon peak position of the synthesized copper nanostructures. When the current was set at 50, 90, and 160 mA, surface plasmon bands were observed at 590, 616, and 626 nm,

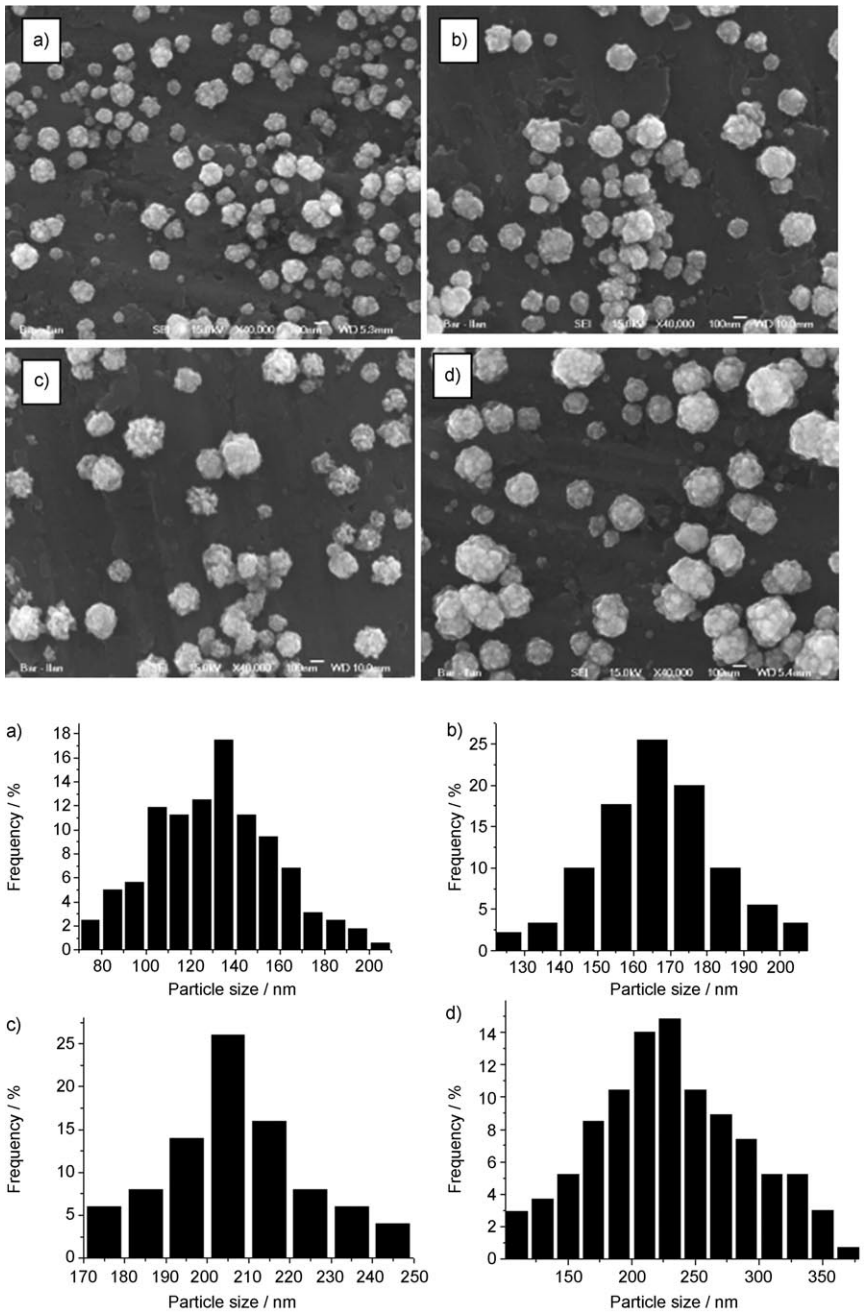

Figure 4. SEM images (top) of the electrode surface after one electric pulse and related size distribution plots (bottom) of individual copper particles at different pulse widths: a) 300, b) 400, c) 600, and d) 800 ms

Table 1. Effect of current pulse width on the size of a copper particles.[a]

Current pulse width [ms]	Flower width [nm]	Flower height [nm]	Particle size [nm]
300	135±10	110±10	33±2
400	165±10	135±10	35±2
600	205±10	155±10	37±3
800	230±20	190±20	44±1

[a] Current = 160 mA.

respectively (Figure 6). The most pronounced plasmon peak was observed at 160 mA, whereas at 50 mA, it was hardly seen at all. The dispersed copper particles were stable for half a day, after which time a red precipitate was detected at the bottom of the flask. To explain the dependence of the plasmon peak position on the pulse current, whilst acknowledging that the plasmon absorption depends on the particle size,[14] we measured the SEM image of the electrode surface after one electric pulse. These measurements were carried out at a constant pulse width of 300 ms, only varying the current to 160, 90, and 50 mA, identical to the currents used for the plasmon measurements. We have found that as the current decreases, the size of the copper nanoparticles increases. According to Table 2, stronger currents led to smaller flowers and smaller nanoparticles. Similar results on current variations with particle size were observed by Rodriquez-Sanchez et al.[16] and in our previous paper on Cu–PVP.[14]

We can thus conclude that at a current of 160 mA, which creates the smallest nanoparticles, the lowest-energy plasmon band (626 nm) is measured. To explain the dependence of the plasmon peak position on the morphology, whilst acknowledging that plasmon absorption depends on the nanostructure, we have measured TEM images taken for the same three currents. The TEM measurements showed a dendritic morphology at a current of 160 mA, whereas for currents of 90 and 50 mA, spherical morphology was detected (Table 2). From the data in Table 2 and Figure 6, we can attribute the absorption peak that appeared at 626 nm to a dendritic nanostructure and the absorption peaks at 590 and 616 nm to the spherical morphology. The dendritic nanostructure shifts absorption to the red region of the spectrum. Zhu et al. observed similar results for Ag dendrites.[6a] Whereas Ag dendrites revealed a plasmon band at 413 nm, the spherical Ag particles showed an absorption band at 383 nm.

The second sonoelectrochemical parameter controlling particle size is the current pulse width. All the other experi-

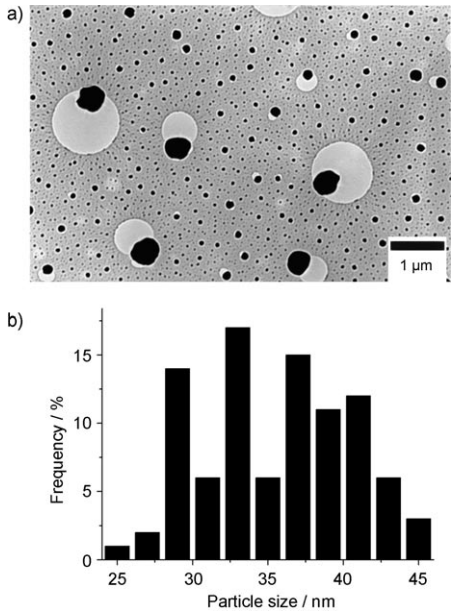

Figure 5. a) TEM image on a gold substrate grid. The copper nanoparticles were synthesized at a current pulse width of 300 ms. b) A histogram of the sizes of individual copper particles.

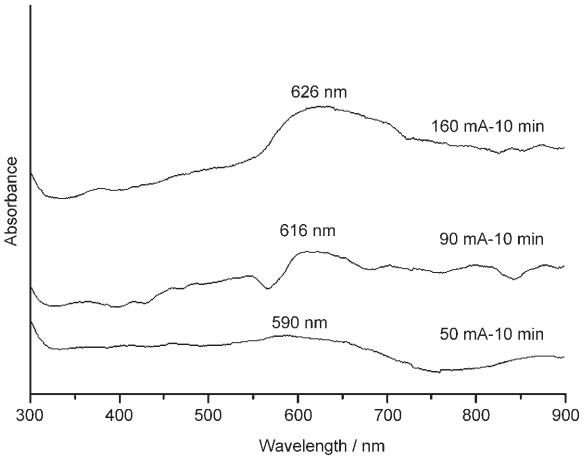

Figure 6. UV/Vis spectra of copper nanoparticles synthesized at different currents with indentical current pulse width conditions (300 ms)

Table 2. Effect of current variation on the copper particle size and morphology[a].

Current [mA]	Flower width [nm]	Flower height [nm]	Particle size [nm]	Surface plasmon band[nm]	TEM morphology
160	135±10	110±10	33±2	626	dendrites
90	250±10	110±10	60±2	616	spherical
50	600±20	110±10	115±3	589	spherical

[a] Current pulse width = 300 ms

mental conditions were kept constant. When the current pulse width was varied, the copper-nanoparticle morphology changed (Figures 1 and 7). The two main structures of the copper product that were obtained from sonoelectrochemical syntheses had dendritic (Figure 1), and dense-wire morphologies (Figure 7a,b). A dendrite morphology was observed for current pulse widths in the range of 300–400 ms, whereas for current pulse widths between 600 and 800 ms, we obtained a dense wire morphology. The length of the dense wires was ≈2 μm, and their width varied between 20 and 50 nm. Figure 8a,b presents a closer look at the dense-wire morphology, which was obtained with an 800 ms current pulse width. These wires consist of small copper particles the sizes of which are around (2.5±0.5) nm. In the magnified image in Figure 8 b, we clearly observe that small copper particles are embedded in a 2 μm polymer strip. We detect the PVA wire, an organic molecule, in the TEM image because of the dispersion of small clusters of copper in the PVA layer.

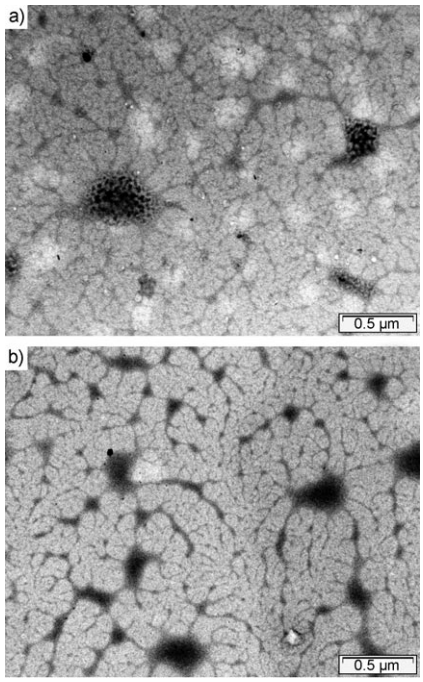

Figure 7. TEM image of the dendrite morphology observed for current pulse widths of a) 600 and b) 800 ms in the presence of PVA.

The next parameter that was examined was the sonoelectrochemical parameter that controls the copper nanoparticle concentration. The nanoparticle concentration is expressed by different time periods of the sonoelectrochemical experiment (the current pulse width is kept constant at 300 ms). The results showed dendritic morphology at run times of 5, 10, 20, and 30 min. The spherical morphology was observed at 2 min. The molar ratios of Cu^0/PVA were 0.91:1, 0.038:1, 0.019:1, 0.009:1, and 0.006:1 for experimental times of 2, 5, 10, 20, and 30 min, respectively.

The origin of dendrite formation: The dendritic structure formed in this research is attributed to the capping agent, PVA. The above experiments clearly show that dendrites are not formed on the electrode. The experiments also reveal that upon removal of the flowers from the electrode

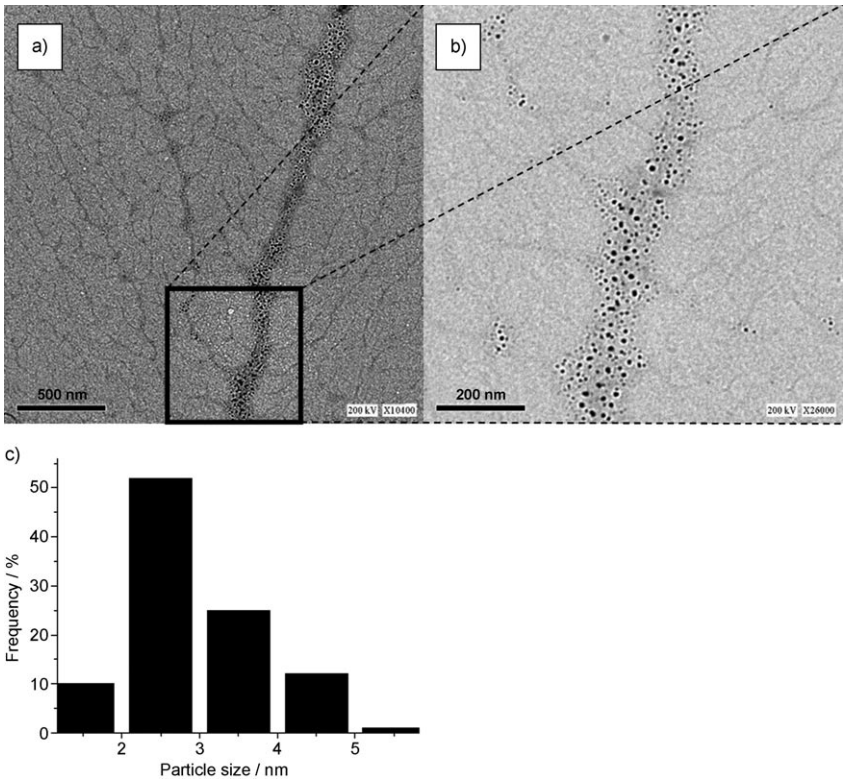

Figure 8. a) and b) TEM images of copper dendrites synthesized at a current pulse width of 800 ms. c) A histogram of the sizes of individual copper particles.

surface, they most probably disintegrate into individual nanoparticles in the solution. The PVA skeleton forms wire- or fingerlike structures that encapsulate the copper nanoparticles. The suggested stabilization mechanism of the copper is similar to that which we presented for the stabilization of spherical copper particles in PVP,[14] although the Cu–PVA aqueous solution is less stable (12 h) than the Cu–PVP solution (48 h). We propose that a chemical interaction between PVA and copper ions takes place through the oxygen of the PVA, which contributes electron density to the vacant orbital of the copper ions. Thereafter, when the current pulse is applied, Cu^{2+} is reduced to Cu^0 on the polymer. The same mechanism is also suggested for the stabilization of Ag by PVA.[17] When we compare the interactions of PVP and PVA with the particles we find that PVP has a stronger interaction than PVA because of the spherical nanoparticles that are formed. PVP shields the nanoparticles, and there are no interactions between the neighboring nanoparticles. PVA dendrites result from interactions between neighboring nanoparticles.

We have demonstrated above that dendrites are not formed on the electrode and most probably not in the solution either. SEM measurements of the electrode after one electric pulse proved the first claim (dendrites did not form on the electrode), whereas the TEM image on the gold grid verifies the second argument (dendrites did not form in the solution). In fact, the independence of the fractal dimension (D) on the duration of the experiment, and on the pulse width, was perhaps also a hint that the dendrites are not related at all to any of the experimental parameters, as shown in the Cu–PVP paper.[14] The above experiments indicated that the dendrites are formed at a later stage, that is, when the metal-colloidal solutions are deposited on the carbon/copper grid under specific sonoelectrochemical parameters.

Dendrite formation depends on the following sonoelectrochemical parameters: the concentration of the Cu nanoparticles and the size of the copper nanoparticles. These two parameters and the nature of the substrate influence the surface evaporation conditions. Our experimental results seem to be consistent with predictions made by Rabani and co-workers.[13] By using a coarse-grained lattice gas model that explicitly accounts for the evaporating solvent, they demonstrated how the nanoparticle size and/or nanoparticle concentration and/or different substrates determine the various morphologies of the final structures.

In our first experiments, we varied particle size, and this parameter influenced nanoparticle diffusion. Smaller particles will, therefore, form a wirelike structure, whereas bigger nanoparticles that move more slowly will form dendrites. This correlates with Yosef and Rabani's theory.[13b] The nanoparticle concentration was the second parameter that was varied. In another paper, Rabani et al.[13a] chose another route and analyzed the importance of the coverage (i.e. mean surface density) and mobility of nanoparticles in determining the morphology of an evaporated solution. At low coverage, disklike aggregates of nanoparticles dominate the self-assembly, namely, the spherical morphology. At high surface coverage, nanoparticle domains are anisotropic, namely, they have a dendritic shape. This is in line with our results, which showed that lower copper nanoparticle concentrations produced spherical particles, and for larger concentrations of nanoparticles, a dendritic morphology was detected.

The last important parameter for dendrite formation that we considered was the nature of the substrate. We interpreted our results in the following way: When the solvent evaporates from the metal surface, spherical or dendrite domains form at different stages. We argue that different substrates allow different evaporation conditions. Thus, because evapo-

ration of the solvent from the gold surface is faster, spherical morphologies are observed, whereas slow evaporation from the copper grid enables dendrite formation.

Conclusions

The synthesis of metallic copper nanostructures by a pulsed sonoelectrochemical method is presented. Polyvinyl alcohol was used as a stabilizing agent. We have investigated the conditions of sonoelectrodeposition, which favor the production of copper with dendritic morphologies. This research has, for the first time, been able to provide an image of the morphology of the copper formed on the electrode after one electric pulse. It also demonstrated that the subsequent sonic pulse removes the copper completely from the electrode surface, cleaning it for the next step. We have monitored the formation of copper dendrites from this early stage of the first electric pulse through the solution. An explanation was offered for dendrite formation as a function of the sonoelectrochemical parameters. This interpretation was based on the coarse-grained model developed by Rabani and co-workers.

Experimental Section

The sonoelectrochemical device employed in the present study was similar to that used by Reisse et al.[14,18,19] A brief description of a sonoelectrochemical setup is given as follows. The titanium horn (ultrasonic liquid processor VC-600, 20 kHz, Sonics & Materials) produced a sonic pulse that was triggered immediately after a current pulse. Two independent pulse drivers were used to control potential and ultrasonic pulses. Spiral platinum wire (0.5 mm diameter and 15 cm long) was used as a counter electrode. The electrolyte consisted of $CuSO_4 \cdot 5H_2O$ (0.16 M) and H_2SO_4 (1.84 M). PVA (1%; $M = 100\,000$) was added to the electrolytes in distilled water (60 mL). The copper deposition was carried out in the electrochemical cell for typically 10–30 min. The anode and cathode of the electrochemical cell were separated by sintered glass. The pulse width of the current was 300 ms and the duration of the ultrasonic pulse was 250 ms. The current of the reaction was kept constant. Morphology and structure investigations were carried out by using a JEOL-JEM 100SX TEM with an accelerating voltage of 80 kV. HRTEM images were taken by using a JEOL 2010 instrument with an accelerating voltage of 200 kV. Samples for TEM and HRTEM were prepared by placing two drops of the dispersed nanoparticle solution on a copper/carbon grid (400 mesh) or on a gold grid (400 mesh), and were then dried under air. A Scion Image software program was used to measure the distribution of particle size by measuring 150–200 particles from the TEM image. A Fractal Dimension software program that has been described previously[20] was used to calculate the dendrite dimensions from the TEM image. The fractal dimension was determined by the "Box Counting" method. A grid of squares was drawn over the fractal area and the number of squares covering the fractal area $S(L)$ was counted. Increasingly smaller squares (side length $L_1, L_2, \ldots L_m$) were used and the number of covering squares ($S(L_1), S(L_2), \ldots S(L_m)$) were counted. The curve is described by the equation $S(L) \approx L^{-D}$, in which D is the fractal dimension value. The XRD pattern of the product was measured with a Bruker AXS D8 Advance Powder X-ray diffractometer (with $Cu_{K\alpha} = 1.5418$ Å radiation). The atomic force microscopic analysis was carried out by using a DI-Digital Instrument Nanoscope Dimension 3100 controller. Optical images were recorded with an Olympus BX51ColorView Soft Imaging System. High-resolution SEM (HRSEM) images were obtained by using a LEOGemini 982 field emission gun SEM (FEG-SEM), which operated at an accelerating voltage of 15 kV. The samples were not sputter-coated with gold prior to imaging. The UV/Vis absorption spectra were recorded on a Perkin–Elmer UV/Visible spectrophotometer and a Cary 1E surface area analyzer. The surface area was measured with a Micromeritics Gemini 2375 analyzer after the samples had been heated at 120 °C for 1 h. The specific surface area was calculated from the linear part of the BET plot at −196 °C.

Acknowledgements

This work was carried out with the support of the European Community Sixth Framework Program through a STREP grant to the SELECTNANO Consortium, Contract No. 516922.03/25/2005. The authors also thank Dr. Y. Grinblat and Dr. T. Tamari for the HRTEM and TEM analyses. We are thankful for Prof. S. Havlin from the Minerva Center and Department of Physics, Bar-Ilan University for the fractal dimension calculation software program.

[1] a) A. P. Alivisatos, *Science* **1996**, *271*, 933; b) T. S. Ahmadi, Z. L. Wang, T. C. Green, A. Henglein, M. A. El-Sayed, *Science* **1996**, *272*, 1924; c) X. Duan, Y. Huang, Y. Cui, J. Wang, C. M. Lieber, *Nature* **2001**, *409*, 66; d) M. B. Mohamed, V. Volkov, S. Link, M. A. El-Sayed, *Chem. Phys. Lett.* **2000**, *317*, 517; e) J. H. Fendler, F. C. Meldrum, *Adv. Mater.* **1995**, *7*, 607.
[2] A. Sukhanova, Y. Volkov, A. L. Rogach, A. V. Baranovi, A. S. Susha, D. Klinov, V. Oleinikov, J. H. M. Cohen, I. Nabiev, *Nanotechnology* **2007**, *18*, 185602.
[3] a) R. Xu, D. Wang, J. Zhang, Y. Li, *Chem. Asian J.* **2006**, *1*, 888; b) K. H. Park, K. Jang, H. J. Kim, S. U. Son, *Angew. Chem.* **2007**, *119*, 1170; *Angew. Chem. Int. Ed.* **2007**, *46*, 1152; c) N. N. Mallikarjuna, R. S. Varma, *Cryst. Growth Des.* **2007**, *7*, 686.
[4] H. Bonnemann, R. M. Richards, *Eur. J. Inorg. Chem.* **2001**, 2455.
[5] a) Y. Zhou, S. H. Yu, C. Y. Wang, X. G. Li, Y. R. Zhu, Z. Y. Chen, *Adv. Mater.* **1999**, *11*, 850; b) A. L. Rogach, V. N. Khvalyuk, V. S. Gurin, *Colloid J.* **1994**, *56*, 221.
[6] a) J. Zhu, S. Liu, O. Palchik, Y. Koltypin, A. Gedanken, *Langmuir* **2000**, *16*, 6396; b) Y. Socol, O. Abramson, A. Gedanken, Y. Meshorer, L. Berenstein, A. Zaban, *Langmuir* **2002**, *18*, 4736.
[7] a) Y. Zhu, H. Zheng, Y. Li, L. Gao, Z. Yang, Y. Qian, *Mater. Res. Bull.* **2003**, *38*, 1829; b) X. Wang, H. Itoh, K. Naka, Y. Chujo, *Langmuir* **2003**, *19*, 6242.
[8] S. T. Selvan, *Chem. Commun.* **1998**, 351.
[9] Y. Song, Y. Yang, C. J. Medforth, E. Pereira, A. K. Singh, H. Xu, J. B. Jiang, C. J. Brinker, F. van Swol, J. A. Shelnutt, *J. Am. Chem. Soc.* **2004**, *126*, 635.
[10] X. F. Qiu, J. Z. Xu, J. M. Zhu, J. J. Zhu, S. Xu, H. Y. Chen, *J. Mater. Res.* **2003**, *18*, 1399.
[11] a) Y. Sawada, A. Dougherty, J. P. Gollub, *Phys. Rev. Lett.* **1986**, *56*, 1260; b) C. M. Lopez, K. S. Choi, *Langmuir* **2006**, *22*, 10625.
[12] a) E. Ben-Jacob, P. Garik, *Nature* **1990**, *343*, 523; b) R. M. Brady, R. C. Ball, *Nature* **1984**, *309*, 225; c) C. Wang, J. Lei, C. Bjelkevig, S. Rudenja, N. Magtoto, J. Kelber, *Thin Solid Films* **2003**, *445*, 72; d) B. K. Sun, T. J. O'Keefe, *Surf. Coat. Tech.* **1998**, *106*, 44; e) S. Gorai, D. Ganguli, S. Chaudhuri, *Mater. Lett.* **2005**, *59*, 826.
[13] a) E. Rabani, D. R. Reichman, P. L. Geissler, L. E. Brus, *Nature* **2003**, *426*, 271; b) G. Yosef, E. Rabani, *J. Phys. Chem. B* **2006**, *110*, 20965; c) C. G. Sztrum, O. Hod, E. Rabani, *J. Phys. Chem. B* **2005**, *109*, 6741; d) C. G. Sztrum, E. Rabani, *Adv. Mater.* **2006**, *18*, 565.
[14] I. Haas, S. Shanmugam, A. Gedanken, *J. Phys. Chem. B* **2006**, *110*, 16947.
[15] a) J. P. Wilcoxon, R. L. Williamson, R. Baughman, *J. Chem. Phys.* **1993**, *98*, 9933; b) C. M. Liu, L. Guo, H. B. Xu, Z. Y. Wu, J. Weber, *Microelectron. Eng.* **2003**, *66*, 107.
[16] L. Rodriguez-Sanchez, M. C. Blanco, M. A. Lopez-Quintela, *J. Phys. Chem. B* **2000**, *104*, 9683.

[17] a) P. K. Khanna, N. Singh, S. Charan, V. V. V. S. Subbarao, R. Gokhale, U. P. Mulik, *Mater. Chem. Phys.* **2005**, *93*, 117; b) Z. H. Mbhele, M. G. Salemane, C. G. C. E. Van Sittert, J. M. Nedeljkovic, V. Djokovic, A. S. Luyt, *Chem. Mater.* **2003**, *15*, 5019; c) B. Karthikeyan, *Physica, B,* **2005**, *364*, 328.

[18] a) J. Reisse, T. Caulier, C. Deckerkheer, O. Fabre, J.; J. Vandercammen, J. L. Delplancke, R. Winand, *Ultrason. Sonochem.* **1996**, *3*, s147; b) A. Durant, J. L. Delplancke, R. Winand, J. Reisse, *Tetrahedron Lett.* **1995**, *36*, 4257; c) J. Reisse, H. Francois, J. Vandercammen, O. Fabre, A. Kirsch-de mesmaeker, C. Maerschalk, J. L. Delplancke, *Electrochim. Acta* **1994**, *39*, 37.

[19] I. Haas, A. Gedanken, *Chem. Mater.* **2006**, *18*, 1184.

[20] A. Bunde, S. Havlin, in *Fractals in Science* (Eds.: A. Bunde, S. Havlin), Springer, Berlin, **1994**, pp. 1–24.

Received: November 6, 2007
Published online: April 2, 2008

